optica

Diode-pumped mid-infrared fiber laser with 50% slope efficiency

Yigit Ozan Aydin,[1,*] Vincent Fortin,[1] Frédéric Maes,[1] Frédéric Jobin,[1] Stuart D. Jackson,[2] Réal Vallée,[1] and Martin Bernier[1]

[1]Centre d'optique, photonique et laser (COPL), Université Laval, Québec G1V 0A6, Canada
[2]MQ Photonics, Department of Engineering, Faculty of Science and Engineering, Macquarie University, North Ryde, NSW 2109, Australia
*Corresponding author: yigit-ozan.aydin.1@ulaval.ca

Received 18 October 2016; revised 16 January 2017; accepted 16 January 2017 (Doc. ID 278990); published 13 February 2017

Until now, the field of mid-infrared fiber laser research has been constrained by the limitation imposed by the Stokes efficiency limit. The conversion of high-power diode light emission operating at near-infrared wavelengths into mid-infrared light invariably results in the deposition of significant amounts of heat in the fiber. This issue is compounded by the fact that mid-infrared transmitting glasses are thermomechanically weak, which means scaling the output power has been a longstanding challenge. In this report, we show that by cascading the adjacent transitions of the erbium ion at 2.8 and 1.6 μm in combination with a low-loss fluoride fiber, the slope efficiency for emission at 2.8 μm can reach 50%, thus exceeding the Stokes limit by 15%. We also show that by highly resonating the 1.6 μm transition, a highly non-resonant excited-state absorption process efficiently recycles the excitation back to the upper laser level of the mid-infrared transition. This demonstration represents a significant advancement for the field that paves the way for future demonstrations that will exceed the 100 W power level.

OCIS codes: (140.3070) Infrared and far-infrared lasers; (140.3500) Lasers, erbium; (140.3510) Lasers, fiber; (060.3735) Fiber Bragg gratings.

https://doi.org/10.1364/OPTICA.4.000235

Fiber lasers emitting in the high-energy portion of the mid-infrared (MIR) at around 3 μm have received significant attention in the past few years as a result of their potential for a vast number of applications in spectroscopy [1], biological tissue ablation [2], and infrared countermeasures [3]. Fiber lasers offer a number of important advantages over other MIR laser technologies resulting from their unmatched beam quality in addition to their compactness, long-term reliability, and great potential for power scaling [4].

The most convenient way to achieve laser emission near 3 μm is to utilize the $^4I_{11/2} \rightarrow {}^4I_{13/2}$ transition of erbium-doped fluoride glass by direct pumping of the $^4I_{11/2}$ level using 976 nm commercial InGaAs laser diodes (see Fig. 1). Achievement of a high slope efficiency is challenging because the quantum defect between the pump and the laser photon limits the maximum conversion efficiency to approximately 35%. In addition, the transition is potentially self-terminating because the lower state ($^4I_{13/2}$) has a longer lifetime than the upper laser level ($^4I_{11/2}$). Several strategies have been developed to reduce the potential of self-saturation of the output: for example, using heavily doped fibers to promote energy transfer upconversion (ETU 1 in Fig. 1, which can recycle the excitation back to the upper laser level) [5–7] or co-doping the fiber with Pr^{3+} de-sensitizer ions that resonantly transfer lower laser level excitation back to the ground state [8]. Cascade lasing at 2.8 μm ($^4I_{11/2} - > {}^4I_{13/2}$) and 1.6 μm ($^4I_{13/2} - > {}^4I_{15/2}$) [9,10] is another promising solution to effectively depopulate the lower state of the 2.8 μm transition, with the significant advantage of reducing the heat generated by avoiding excitation to higher states and using photon emission down to the ground state.

Optical-to-optical conversion efficiencies of 3 μm-class Er^{3+}-fluoride fiber lasers have been significantly improved recently by using high-quality low-loss and heavily doped erbium fibers to take advantage of the ETU 1 process. The first experimental evidence of pump recycling through ETU 1 was observed in a single-mode laser cavity that generated 20.6 W at a wavelength of 2.825 μm [5]; however, the slope efficiencies barely exceeded the Stokes limit and were far from reaching the predicted values of >50% for the erbium system at high doping concentrations [11]. Recently, Li *et al.* [10] reported a cascaded erbium-doped fiber laser based on a lightly Er^{3+}-doped (1.5 mol. %) fluoride fiber to produce efficiencies of 26.7% and 7.1% with respect to the absorbed pump powers of the 2.8 μm and 1.6 μm emissions, respectively. Overall, it has been widely understood that the slope efficiency could only be exceeded by exploiting the ETU in heavily doped fibers, which forces heat loads per unit length of the fiber that will certainly lead to problems in future power scaling attempts [6].

In this Letter, we report a highly efficient and passively cooled erbium-doped fluoride fiber laser operating at the 10 W level based on the cascade lasing scheme that sets a new slope efficiency record of 50% at the 2.8 μm emission wavelength with respect to absorbed pump power at 976 nm. The presence of an excited-state

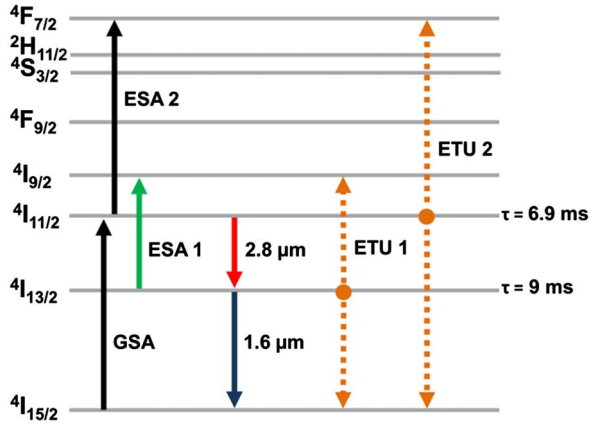

Fig. 1. Partial energy level diagram of the relevant energy states of the erbium ions in fluoride glasses. ESA 2 corresponds to the ESA process introduced in this Letter.

absorption (ESA) band centered at 1.675 μm between the $^4I_{13/2}$ and $^4I_{9/2}$ levels, which partially overlaps the cascaded emission at 1.614 μm, is observed and is believed to be responsible for the recycling of the excitation back to the upper laser level. One of the key features to result from this study is the need to highly resonate the emission from the lower transition of the cascade to maximize the efficiency at 2.8 μm.

In the preliminary experiments, we used a simple fiber laser arrangement and different lengths of a gain fiber (3, 7, and 10 m) to study the efficiency dependence on the length of the cascaded outputs. The experimental setup of the cascade laser is shown in Fig. 2. The gain of the laser cavity is provided by an erbium-doped zirconium fluoride fiber from Le Verre Fluoré, France. The core had a 16.5 μm diameter, a numerical aperture (NA) of 0.12, and an erbium concentration of 1 mol. %. The propagation losses were measured to be less than 40 dB/km at 2.8 μm. The cladding had a 260 μm diameter (a circular shape with two parallel flats) and was coated with a low-index fluoroacrylate polymer to allow pump guiding with an NA of >0.46. The cladding pump absorption at 976 nm was approximately 0.3–0.35 dB/m, and the background losses were less than 0.1 dB/m at 976 nm.

The active fiber was pumped by two multimode laser diodes (IPG PLD-33) operating at approximately 976 nm, and each delivered up to 30 W in 105/125 μm, 0.12 NA silica fibers. A multipump combiner (ITF Technologies) with the same input fibers was used to combine the pump power into a 220/242 μm, 0.22 NA silica fiber. The input tip of the Er^{3+}-fluoride glass

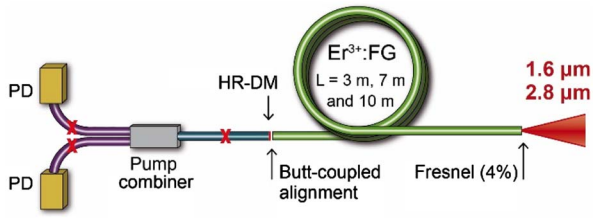

Fig. 2. Experimental setup of the cascade laser operating at ~2.8 and ~1.6 μm that was used to test the performance against different gain fiber lengths (3, 7, and 10 m). Fresnel reflection was used for feedback. HR-DM, highly reflective dichroic mirror; PD, pump diode.

(Er^{3+}:FG) fiber was cleaved perpendicular to the axis of the fiber and was butt coupled to the output fiber of the combiner using a μm-resolution three-axis stage with copper V-grooves. The cleave angles of fibers were kept below 1° using an optimized cleave recipe to ensure butt coupling with a minimum air gap.

The laser cavity was made on one end of a highly reflective dichroic mirror (HR-DM) having a reflectivity of ~80% at both 1.6 and 2.8 μm and a transmission of more than 90% around 976 nm. The HR-DM was deposited on the tip of the output fiber of the combiner and consisted of a multilayer coating made of Ta_2O_5 and SiO_2, as described in [12]. At the other end of the Er^{3+}:FG fiber, a Fresnel reflection from a straight cleaved endface acted as the output coupler for both wavelengths.

The output powers of the laser and residual pump were monitored with a thermopile detector (Gentec, UP19K-30H-H5) in combination with two different dichroic mirrors to isolate the 976 nm, 1.6 μm, and 2.8 μm power levels. Figure 3 shows the measured output power of both cascaded transitions as a function of the launched and the absorbed pump power for the three different lengths of gain fiber tested.

The maximum launched pump power at 976 nm was limited to approximately 25 W for all setups. In some experiments, self-pulsing at 2.8 μm was observed in the vicinity of the 1.6 μm lasing threshold. These instabilities were most problematic for the 10 m

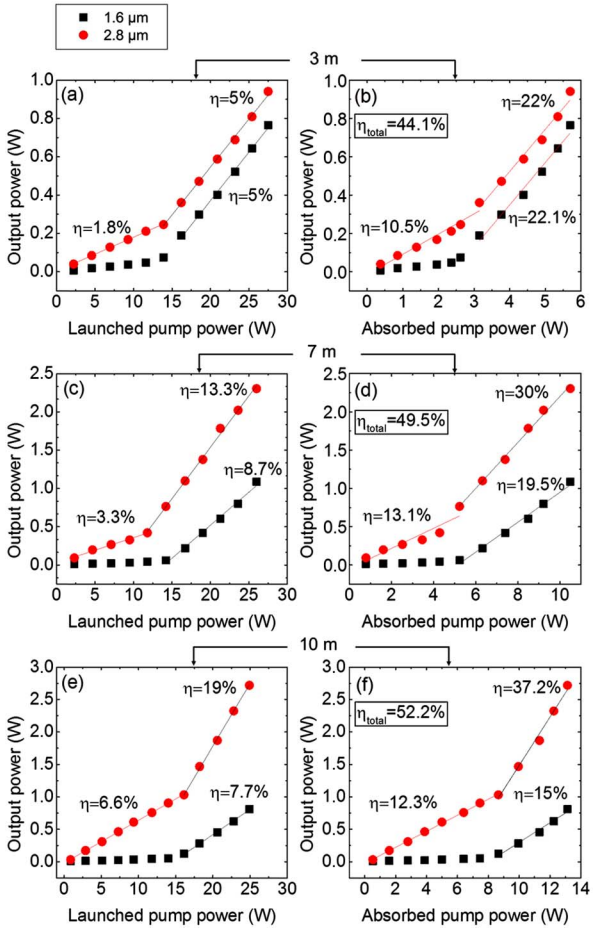

Fig. 3. Measured output power with respect to the launched and absorbed pump powers for cavity lengths of (a), (b) 3 m, (c), (d) 7 m, and (e), (f) 10 m. The black and red dots, respectively, refer to 1.6 and 2.8 μm emissions.

length experiment, since they resulted in catastrophic failures along points in the fiber core as the 1.6 μm lasing threshold was reached at a high pump power. We believe this might be the result of a saturable absorption process from the ground-state Er^{3+} ions located in the un-pumped end of the fiber, which results in giant Q-switched pulse formation at high pump powers [13].

We observe that the 2.8 μm slope efficiency strongly increases after the 1.6 μm transition threshold is reached (in agreement with [10]). Moreover, the threshold of the 1.6 μm transition (versus the absorbed pump power) is reduced as the fiber length is shortened, while its efficiency increases. On the other hand, the combined laser efficiency ($\eta_{\text{total}} = \eta_{1.6\,\mu\text{m}} + \eta_{2.8\,\mu\text{m}}$) slightly increases with the fiber length. The slope efficiency of the 2.8 μm emission above the cascade threshold is observed, for the 10 m fiber length, to surpass the Stokes efficiency limit. Based on these preliminary results, an optimized laser cavity was designed to maximize the laser efficiency for the 2.8 μm transition. For this purpose, a longer fiber has been selected to enhance the 2.8 μm efficiency at the expense of the 1.6 μm efficiency and to absorb a larger portion of the launched pump power. In addition, the total reflectivity of the cavity at 1.6 μm was raised to keep its threshold as low as possible, thus avoiding threshold-related instabilities at high pump levels. The optimized system therefore included fiber Bragg gratings (FBGs) to provide a higher and spectrally controlled feedback. The experimental setup of the optimized cascade laser is shown in Fig. 4.

The laser is made of a 21 m length of active fiber that was identical to the fiber used in the first experiments. The 2.8 μm cavity was bounded by a highly reflective input FBG (HR-FBG) having a maximum reflectivity of ≥ 99.5% centered at 2.825 μm and by the broadband Fresnel reflection from the output endcap face. As for the 1.6 μm cavity, it is composed of an HR-DM deposited on the butt-coupled silica endface with an effective reflectivity of ~80% near 1.6 μm and less than 10% near 2.8 μm, while the HR-FBG had a maximum reflectivity of ≥ 99.5% centered at 1.614 μm. The transmissions of the 976 nm pump through the input dichroic mirror and the HR-FBG at 2.825 μm were ~90% and ~98%, respectively. The FBGs used in this setup have respective FWHM bandwidths of 0.25 nm (HR-FBG at 1.614 μm) and 0.9 nm (HR-FBG at 2.825 μm) and were written directly in the Er^{3+}:FG fiber by a femtosecond laser at 800 nm using a phase mask, as described in [14]. The spectra of both the 1.6 and 2.8 μm signals are presented in the Supplement 1. The polymer coating over the last 10 cm of the erbium fiber was removed in order to apply a UV-cured high-index acrylate polymer ($n = 1.54$) to remove the un-absorbed residual 976 nm pump power. After the experiments were completed, the residual pump stripper was removed to measure the residual pump and to perform a cutback procedure for a precise evaluation of the absorbed pump power.

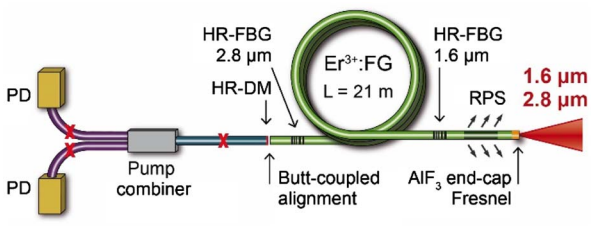

Fig. 4. Experimental setup of the optimized cascade laser operating at 2.825 and 1.614 μm. The cavity is based on a 21 m gain fiber and includes FBGs. HR-DM, highly reflective dichroic mirror at 1.6 μm; RPS, residual pump stripper; PD, pump diode.

A short endcap ($L = 136$ μm) is fabricated on the output tip of the Er-fluoride fiber by splicing an AlF_3-based multimode fluoride fiber (200/220 μm, 0.22 NA), which is then cleaved at a right angle (below 1°) to provide the broadband feedback of 0.5 to 0.75% for the 2.8 μm transition. The fusion splice was achieved with a filament-based splicer (Vytran GPX). AlF_3 endcaps are key components in high-power MIR fiber lasers to reduce the catastrophic optical damage associated with OH diffusion in the fiber tip [15]. The fiber was fixed on an aluminum plate for passive cooling. During the laser operation, the active fiber and the FBGs were also observed with a thermal imaging camera (Jenoptik IR-TCM 640) to anticipate the onset of hot spots in the laser cavity.

The measured output powers with respect to absorbed pump power are shown in Fig. 5. The maximum launched pump power in the active fiber was 43.4 W, corresponding to 52.9 W of pump light delivered from the pump silica fiber (i.e., a ~82% launching efficiency was achieved). As in the preliminary experiments, the slope efficiency of the 2.8 μm laser transition increases significantly when the 1.6 μm threshold is reached, from 16.6% to 49.5% with respect to absorbed pump power. The highest power achieved at 2.825 μm is 12.95 W with negligible (~0.35 W) output power at 1.614 μm.

For most of the pump power range, the spectrum of the 2.8 μm signal was centered on the input FBG (2.825 μm). However, a secondary peak around 2.85 μm was observed for pump power levels near the maximum. This observation is consistent with the strong wavelength shift previously seen in a similar cascaded lasing scheme [10]. Moreover, we observed that the emergence of the second spectral peak triggered temporal instabilities and, in some cases, resulted in pulse formation that could lead to fiber damage at high pump powers. To avoid these problems, the Bragg wavelength of the 2.8 μm FBG will need to be increased. The optimal grating wavelength for such a cascade laser arrangement is still under investigation.

The efficiencies achieved in this study are the highest reported for a diode-pumped 3 μm class fiber laser, but the mechanism underlying the performance is not fully understood. Generally, ESA and energy transfer processes play a vital role in the ion

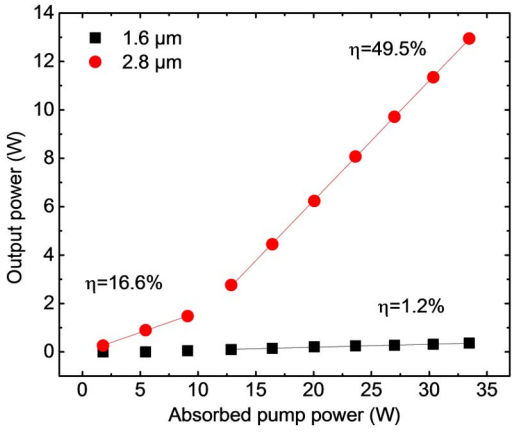

Fig. 5. Measured output powers at 1.6 and 2.8 μm with respect to absorbed pump power for the 21 m fiber length.

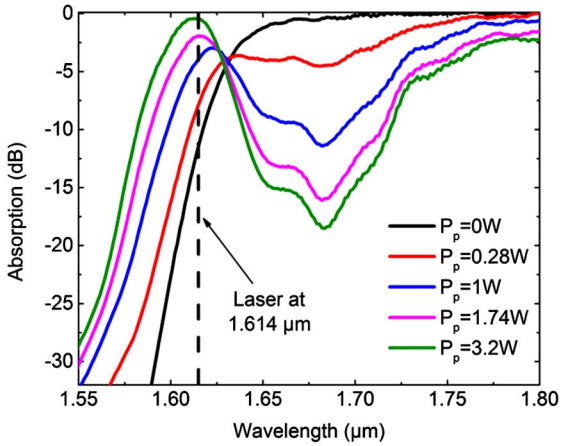

Fig. 6. Absorption spectrum of a 90 cm length of the 1 mol. % Er^{3+}-doped fluoride fiber between 1.55 and 1.80 μm for varying launched pump powers from 0 to 3.2 W.

dynamics of erbium-based fluoride glass systems. In the current fiber, the concentration of Er^{3+} ions (1 mol. %) is believed to be too low for ion–ion interactions to play a major role and hence ESA, enhanced by the presence of high circulating 1.6 μm power in the core of the fiber, may lead to an additional recycling process. In an effort to isolate the mechanism, a pump/probe experiment in which a supercontinuum signal was launched in the Er^{3+}:FG fiber core with and without pumping at 976 nm was carried out (see Supplement 1). An ESA process, centered at 1.675 μm with the high energy portion overlapping the 1.614 μm emission, is identified. It originates from the $^4I_{13/2} \rightarrow {}^4I_{9/2}$ transition (ESA 2 in Fig. 1), which, according to previous spectroscopic measurements [16], would correspond to an energy gap of 5886 cm^{-1} (~1.70 μm photon wavelength). Figure 6 shows the ESA spectrum centered around 1.675 μm, and part of the 1.5 μm ground-state absorption spectrum when a 90 cm length of active fiber is pumped at varying 976 nm pump powers. A maximum ESA of −18.5 dB occurs for a launched pump power of 3.2 W. While this transition has been measured in Er^{3+}:$LiYF_4$ crystals [17], to our knowledge, this is the first time it is observed in an erbium-doped glass.

The proposed process $^4I_{13/2} + h\nu_{1.6\,\mu m} \rightarrow {}^4I_{9/2}$ effectively recycles excitation back to the $^4I_{11/2}$ upper laser level. As a result, a longer gain fiber length increases the ESA of the 1.6 μm signal, leading to an efficiency increase at 2.8 μm.

Experimentally, the butt-coupled pump alignment could be replaced by a fusion splice [7] to obtain a monolithic laser system with enhanced efficiency and reliability. In the current experiment, the erbium fiber length was not optimized because the maximum length of a useful fluoride fiber is limited by scattering centers caused by geometrical defects and crystallization in the fabrication process [18]. Additional efficiency and output power scaling should be possible by extending the active fiber length and optimizing the 1.6 μm emission wavelength according to the ESA cross-section spectrum. The availability of longer defect-free fluoride fibers, combined with the above-mentioned improvement, could lead to output powers at 3 μm reaching the 100 W level.

In summary, a passively cooled cascade Er^{+3}-doped fluoride fiber laser with an output power of ~13 W and a record slope efficiency of 50% at 2.825 μm has been reported. The influence of the 1.6 μm transition on the 2.8 μm efficiency was studied by changing the gain fiber length. The presence of the ESA process around ~1.675 μm suggests that ESA-induced energy recycling may be responsible for significantly increasing the slope efficiency beyond the Stokes limit.

Funding. Natural Sciences and Engineering Research Council of Canada (NSERC) (CG101779, CG112389); Canada Foundation for Innovation (CFI) (GF072345); Fonds de recherche du Québec - Nature et technologies (FRQNT) (CO201310, FT097991); Australian Research Council (ARC) (DP140101336).

Acknowledgment. The authors would like to thank Marc D'Auteuil and Souleymane Toubou Bah for the fabrication of the dichroic mirrors. The authors also thank David Ottaway for the initial discussions associated with excited-state absorption.

See Supplement 1 for supporting content.

REFERENCES

1. F. K. Tittel, D. Richter, and A. Fried, in *Solid-state mid-infrared laser sources*, I. Sorokina and K. Vodopyanov, eds. (Springer, 2003), paper 458.
2. M. C. Pierce, S. D. Jackson, M. R. Dickinson, T. A. King, and P. Sloan, Lasers Surg. Med. **26**, 491 (2000).
3. H. H. P. T. Bekman, J. C. van den Heuvel, F. J. M. van Putten, and R. Schleijpen, Proc. SPIE **5615**, 27 (2004).
4. D. J. Richardson, J. Nilsson, and W. A. Clarkson, J. Opt. Soc. Am. B **27**, B63 (2010).
5. D. Faucher, M. Bernier, G. Androz, N. Caron, and R. Vallée, Opt. Lett. **36**, 1104 (2011).
6. S. Tokita, M. Murakami, S. Shimizu, M. I. Hashida, and S. Sakabe, Opt. Lett. **34**, 3062 (2009).
7. V. Fortin, M. Bernier, S. T. Bah, and R. Vallée, Opt. Lett. **40**, 2882 (2015).
8. P. S. Golding, S. D. Jackson, T. A. King, and M. Pollnau, Phys. Rev. B **62**, 856 (2000).
9. S. D. Jackson, Electron. Lett. **45**, 830 (2009).
10. J. Li, L. Wang, H. Luo, J. Xie, and Y. Liu, IEEE Photon. Technol. Lett. **28**, 673 (2016).
11. M. Pollnau and S. D. Jackson, IEEE J. Quantum Electron. **38**, 162 (2002).
12. V. Fortin, F. Maes, M. Bernier, S. T. Bah, M. D'Auteuil, and R. Vallée, Opt. Lett. **41**, 559 (2016).
13. S. Colin, E. Contesse, P. Le Boudec, G. Stephan, and F. Sanchez, Opt. Lett. **21**, 1987 (1996).
14. M. Bernier, D. Faucher, R. Vallée, A. Saliminia, G. Androz, Y. Sheng, and S. L. Chin, Opt. Lett. **32**, 454 (2007).
15. N. Caron, M. Bernier, D. Faucher, and R. Vallée, Opt. Express **20**, 22188 (2012).
16. Y. D. Huang, M. Mortier, and F. Auzel, Opt. Mater. **17**, 501 (2001).
17. J. Koetke and G. Huber, Appl. Phys. B **61**, 151 (1995).
18. S. D. Jackson, Nat. Photonics **6**, 423 (2012).